ratio 1:3 and Fig. 2c, the decay rates have become independent of the initial boundary-layer thicknesses. The relatively shorter decay distance for the cases in Fig. 2c, compared to those in Figs. 2a and 2b, further showed that a faster mixing rate can be achieved by a larger velocity ratio across the lobe.[5,6]

The results in Fig. 2 also suggested that at thin initial boundary layers, the increase in velocity ratio has actually enhanced the decay rate, see, for example, the 1/10λ case in Figs. 2a–2c. In contrast, the decay rates at various velocity ratios are very similar to each other in the cases of the medium and thick initial boundary layers, see Figs. 2b and 2c. Moreover, in all cases considered here, the strength of the streamwise vorticity has been almost dissipated by 7λ from the trailing edge.

Variation of the streamwise vorticity at velocity ratio 1:3 and an initial boundary-layer thickness of 1/3λ from Ref. 5 have also been plotted in Fig. 2c for comparison. The magnitude is very similar at locations close to the trailing edge, but the decay rate of Ref. 5 becomes asymptote to lower values after 5λ. This may be because of a difference in the freestream turbulence levels in the present case (~0.5%) and that of Ref. 5 (~2%).

The results in the present investigation generally suggested that large velocity ratios and thick initial boundary layers would normally lead to a faster decaying rate. Thus, the decay rate is closely related to the normal vorticity shed at the trailing edge since the strength of the normal vorticity depends on the velocity ratios and initial boundary-layer thicknesses.

Finally, it appears that the initial boundary-layer thicknesses and velocity ratios have no significant influence on the magnitude of the streamwise vorticity near the trailing edge. The results further confirm the analysis of Skebe et al.[4] that the streamwise vorticity at the trailing edge generated by a lobe is indeed inviscidly generated.

Concluding Remarks

The following concluding remarks can be drawn from the preceding text:

1) At thin and medium initial boundary layers, the increase in velocity ratio enhances the streamwise vorticity decay rate with downstream distance.

2) At thick initial boundary layer, the increase in velocity ratio does not significantly change the streamwise vorticity decay rate with downstream distance.

3) At velocity ratios 1:1 and 1:2, the increase in the thickness of the initial boundary layers enhances the streamwise vorticity decay rate with downstream distance.

4) At velocity ratio 1:3, the streamwise vorticity decay rate is independent of initial boundary-layer thicknesses.

5) The trailing-edge streamwise vorticity appears to be independent of initial flow conditions.

Acknowledgments

Financial support for this project from the Academic Research Fund, and the Graduate Scholarship for X. Xu and T. H. Yip from the School of Mechanical and Production Engineering, are gratefully acknowledged.

References

[1]Paterson, R. W., "Turbofan Mixer Nozzle Flow Field—A Benchmark Experimental Study," *Journal of Engineering for Gas Turbines and Powers*, Vol. 106, July 1984, pp. 692–698.

[2]Eckerle, W. A., Sheibani, H., and Awad, J., "Experimental Measurement of the Vortex Development Downstream of a Lobed Forced Mixer," *Journal of Engineering for Gas Turbines and Power*, Vol. 114, Jan. 1992, pp. 63–71.

[3]McCormick, D. C., and Bennett, J. C., Jr., "Vortical and Turbulent Structure of a Lobed Forced Mixer Free-Shear Layer," *AIAA Journal*, Vol. 32, Sept. 1994, pp. 1852–1859.

[4]Skebe, S. A., Paterson, R. W., and Barber, T., "Experimental Investigation of Three-Dimensional Forced Mixer Lobe Flow Fields," AIAA Paper 88-3785, Jan. 1988.

[5]Yu, S. C. M., Yeo, J. H., and Teh, J. K. L., "Velocity Measurements Downstream of Lobed-Forced Mixer with Different Trailing-Edge Configurations," *Journal of Propulsion and Power*, Vol. 11, No. 1, 1995, pp. 87–95.

[6]Manning, T. A., "Experimental Studies of Mixing Flows with Streamwise Vorticity," M.S. Thesis, Massachusetts Inst. of Technology, Cambridge, MA, Sept. 1991.

Experimental Investigation of Angled Injection in a Compressible Flow

Roy J. Hartfield Jr.* and Douglas J. Bayley†
Auburn University, Auburn, Alabama 36849-5338

Introduction

THE mixing characteristics of angled injection have applications in scramjet combustors[1] and in air-augmented ducted rockets. Mixing and mixing enhancement has been investigated for both subsonic[2] (ducted rocket and ramjet) and supersonic[3–7] (scramjet) freestreams. Reference 6 describes measurements of injectant penetration boundaries and visualization results for angled injection. The work presented herein builds on that database with quantitative measurements of injectant mole fraction.

The test section for this investigation is a constant area duct with an angled injector located just downstream of a Mach 2 laval nozzle. The test section is 52 mm long, 10.2 mm wide, and 7.2 mm high. Air injection through a straight 2-mm-diam circular cross section injector is studied for injection angles of 30, 45, and 60 deg measured relative to the top wall of the tunnel. The oblique angle between the injector and the top wall of the test section results in an elliptical injector exit. A jet-induced bow shock is formed immediately upstream of the injector and is reflected through the mixing region of the test section.

Experimental Technique and Setup

The measurement approach employed in this investigation is quantitative imaging of the injectant mole fraction using planar laser-induced iodine fluorescence (PLIIF). The PLIIF measurement technique, described in detail in Ref. 3, involves removing the thermodynamic and geometric dependence of the fluorescence signal. An uncertainty analysis for the experimental setup employed here indicates an expected uncertainty in the measurements of 5% for most of the data.

The experimental facility consists primarily of a small-scale, Mach 2 wind tunnel equipped with fused silica windows, a Spectra Physics model 171 argon-ion laser, a Photometrics Star 1 camera system, and an IBM-compatible 80386 microcomputer. An Ingersoll Rand 250-scfm compressor and a silica-bead desiccant dryer comprise the air supply system. For measurements requiring iodine, air is diverted through a mixing vessel.

Received March 3, 1995; presented as Paper 95-2414 at the AIAA/ASME/SAE/ASEE 31st Joint Propulsion Conference and Exhibit, San Diego, CA, July 10–12, 1995; revision received Oct. 31, 1995; accepted for publication Nov. 3, 1995.

*Assistant Professor, Department of Aerospace Engineering. Member AIAA.

†Graduate Research Assistant; currently Second Lieutenant, U.S. Air Force.

The 4-W laser sheet was generated using a 6-mm focal-length cylindrical lens and a 300-mm focal-length, 7.5-cm-diam spherical lens. A flat mirror, which turns the sheet into the test section, and the camera are mounted on a micrometer-driven translation stage. This setup can be configured for imaging in the penetration plane (parallel to the freestream showing penetration) and in the crossflow plane (perpendicular to the freestream direction). For presentation, the data from the crossflow planes was stretched geometrically in the horizontal direction to compensate for the skewing induced by the 30-deg viewing angle.

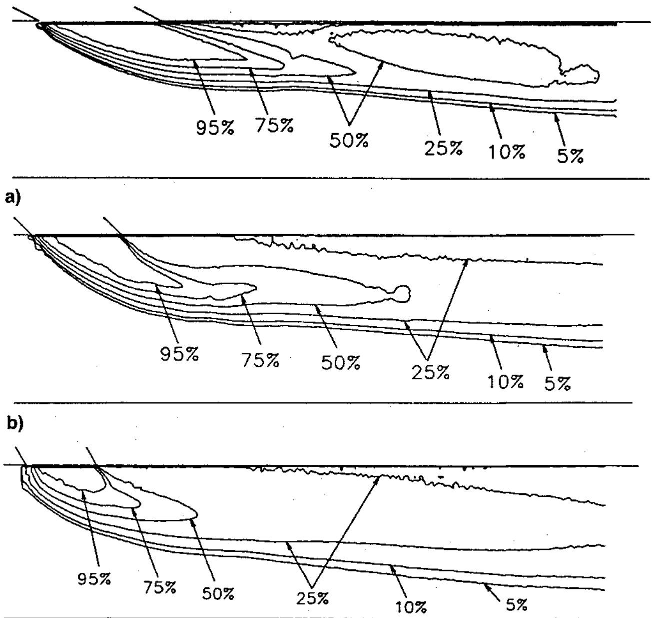

Fig. 1 Injectant mole fraction distributions in the centerline penetration plane: a) 30-, b) 45-, and c) 60-deg injectors.

Results

Contour plots of the injectant mole fraction distribution along the center penetration plane for the three injectors are shown in Fig. 1. The distribution for the 30-deg injector is indicative of the presence of streamwise vorticity formed by the jet's angled blockage of the freestream. The effect of the angled jet is much the same as a physical ramp and the resulting vortex action pulls freestream air into the center of the injectant plume.[4,7] The vortex influence is particularly apparent in the shape of the 50% contour.

For the 45-deg injector, the jet core is smaller than for the 30-deg injector and no downstream region of high-injectant mole fraction is separated from the primary injectant stream by a band of low-injectant mole fraction fluid in this penetration plane. This indicates a lessening of the vortex domination of mixing for 45-deg injection. Note, however, that the injectant is pulled from the top wall and the injectant penetration has increased.

The continued increase in mixing rate with injection angle is clearly seen in the small-sized 95, 75, and 50% contours found in the plot for the 60-deg injector. For this case, the 95% contour barely extends to the edge of the jet and the 50% contour extends only a few jet diameters downstream. Again, the downstream injectant plume is lifted off the top wall.

The injectant mole fraction crossflow contour plots (Figs. 2–4) are presented for planes at injector diameter intervals with X representing the downstream direction and X/D = 0 at the injector center. For both the 30- and 45-deg cases, the area for each crossflow plot covers 52% of the test section width and 68% of the tunnel height. The area of the plots for the 60-deg injector covers 60% of the test section width and 74% of the test section height.

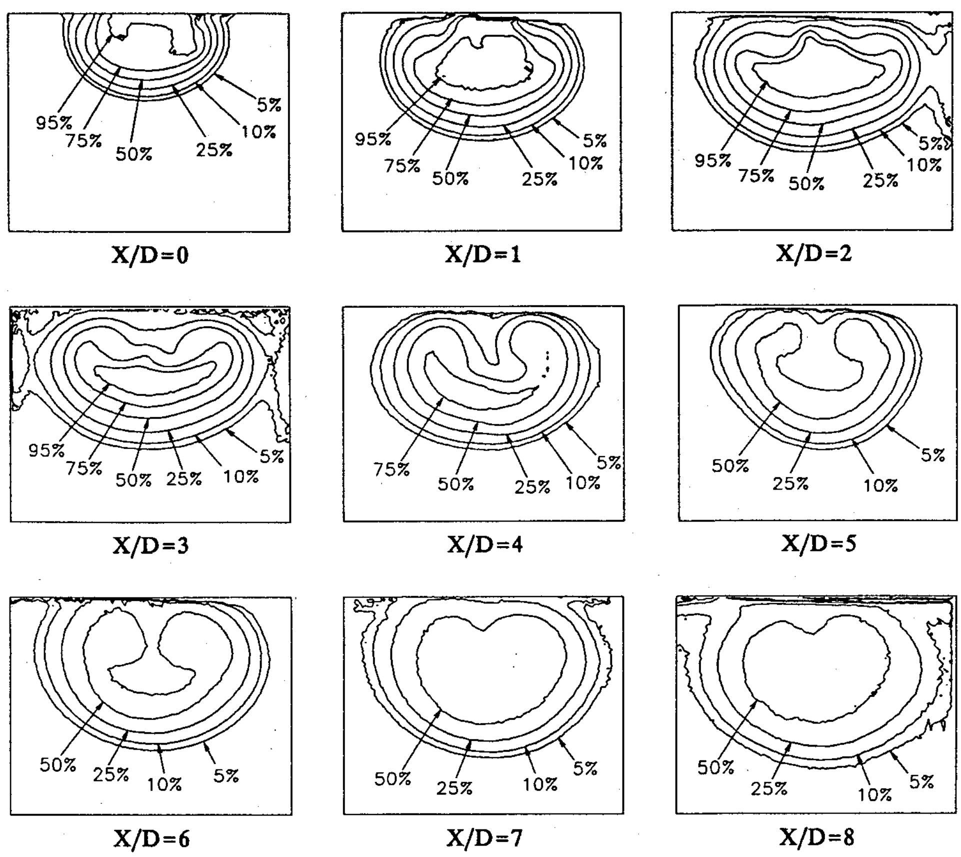

Fig. 2 30-deg injector crossflow injectant mole fraction distribution.

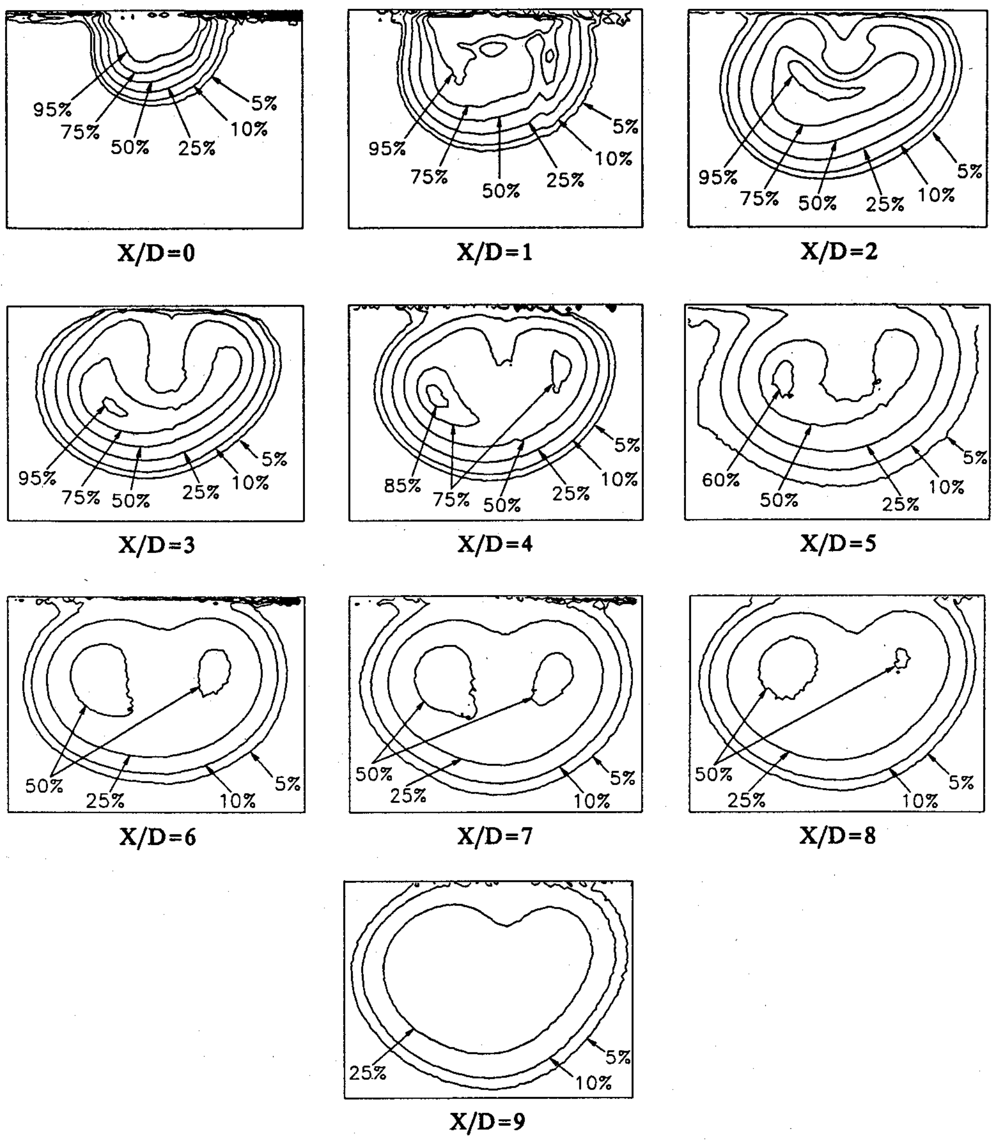

Fig. 3 45-deg injector crossflow mole fraction distribution.

The crossflow injectant mole fraction contour plots for the 30-deg injector are shown in Fig. 2. At X/D = 0, the jet core is present and the effects of the vorticity are not clear. At X/D = 1, the jet core has expanded. For X/D = 2 and X/D = 3, the initial effects of the vorticity can be seen and much stronger effects of the vorticity are clear at X/D = 4, X/D = 5, and X/D = 6. At X/D = 7 and X/D = 8, the lack of a structure in the injectant mole fraction contours indicates that the dominance of the mixing process by the vorticity has ended.

The contour plots of injectant mole fraction for the crossflow planes in the 45-deg injection flowfield are shown in Fig. 3. At X/D = 0 and X/D = 1, the effects of the vortex action are not apparent. Some effects of the vorticity can be seen at X/D = 2 and X/D = 3 as some of the freestream air is drawn into the center. At X/D = 4, the influence of the vorticity on the mixing has been reduced, even though two pockets remain around the 75% contour. At X/D = 5 the 50% contour is a reminder that the vorticity is still present and there is little structural change in the distribution from X/D = 6 to X/D = 9.

The lower influence of the vorticity for the 60-deg injector is evident in the crossflow plots shown in Fig. 4. The effects of the vorticity on the mixing are less evident in these plots than in the plots for the 30- and 45-deg data. The injectant mole fraction distributions for X/D = 0 and X/D = 1 are similar to the corresponding distributions for the other two injectors. (Again, the jet core is contained within the very small 95% contours.) Some signs of vorticity are apparent at X/D = 2 and X/D = 3. The highest plotted contour at X/D = 2 is 75% and at X/D = 3 the highest plotted contour is 50%, which agrees with the contours obtained in the penetration plane and illustrates the dramatically increased mixing rate. The remnants of the vorticity influence remain at X/D = 4 and X/D = 5 in the shrinking 50% contour pockets. For the last four distributions the injectant penetration increases and the jet plume around the 25% contour moves away from the top wall of the test section.

Summary and Conclusions

Injectant mole fraction distributions for the 30-deg injector show considerable vortex domination of the mixing. The 45-deg injector distributions display some signs of vortex domination, but the vortex influence on the mixing is not as developed as for the 30-deg injector. Injectant penetration increased for the 45-deg injector. Even less vortex domination was observed for the 60-deg injector, but the injectant penetration into the freestream increased to approximately 80% of the test section height at the end of the measurement domain. The injectant mole fraction measurements make it quite clear that the mixing in the near field of the injector is dominated by large vortices in the freestream, particularly for lower injection angles. Further research into the mixing of angled jets should

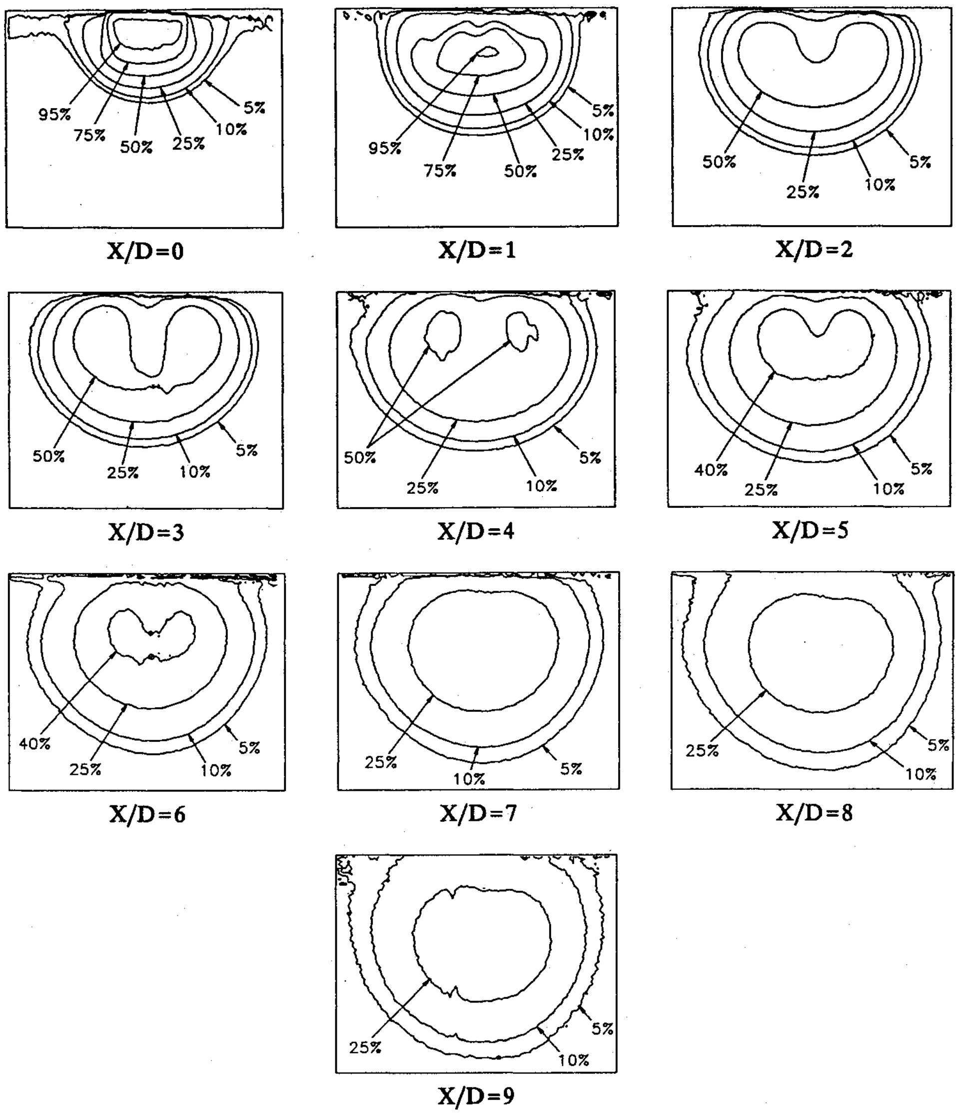

Fig. 4 60-deg injector crossflow injectant mole fraction distribution.

include efforts to quantify the tradeoff between total pressure loss and increases in mixing rate.

References

[1]Waltrup, P. J., "Liquid-Fueled Supersonic Combustion Ramjets: A Research Perspective," *Journal of Propulsion and Power*, Vol. 3, No. 6, 1987, pp. 515–524.

[2]Cherng, D. L., Yang, V., and Kuo, K. K., "Numerical Study of Turbulent Reacting Flows in Solid-Propellant Ducted Rocket Combustors," *Journal of Propulsion and Power*, Vol. 5, No. 6, 1989, pp. 678–685.

[3]Hartfield, R. J., Abbitt, J. D., and McDaniel, J. C., "Injectant Mole Fraction Imaging in Compressible Mixing Using Planar Laser-Induced Iodine Fluorescence," *Optics Letters*, Aug. 15, 1989, pp. 850–852.

[4]Riggins, D. W., Mekkes, G. L., McClinton, C. R., and Drummond, J. P., "A Numerical Study of Mixing Enhancement in a Supersonic Combustor," AIAA Paper 90-0203, Jan. 1990.

[5]Schetz, J. A., Thomas, R. H., and Billig, F. S., "Mixing of Transverse Jets and Wall Jets in Supersonic Flow," *Separated Flows and Jets*, edited by V. V. Koslow and A. V. Dovgal, Springer–Verlag, Berlin, 1991.

[6]Gruber, M. R., Nejad, A. S., Chen, T. H., and Dutton, J. C., "Mixing and Penetration Studies of Sonic Jets in a Mach 2 Freestream," AIAA Paper 94-0709, Jan. 1994.

[7]Hartfield, R. J., Hollo, S. D., and McDaniel, J. C., "Experimental Investigation of a Supersonic Swept Ramp Injector Using Laser-Induced Iodine Fluorescence," *Journal of Propulsion and Power*, Vol. 10, No. 1, 1994, pp. 129–135.

Theoretical Upper Limits on Enthalpy Rocket Performance

Timothy W. Parker* and Ronald W. Humble†
University of Colorado, Colorado Springs, Colorado 80918

Nomenclature

A, B = intermediate variables for integration
A_t = nozzle throat area, m^2

Presented as Paper 94-2872 at the AIAA 30th Joint Propulsion Conference, Indianapolis, IN, June 27–29, 1994; received Sept. 16, 1994; revision received Oct. 3, 1995; accepted for publication Oct. 4, 1995.

*Masters Student; currently Captain in U.S. Air Force, Undergraduate Space and Missile Training Instructor, 1472 Nevada Avenue, Suite 252, Vandenberg Air Force Base, CA 93437-5329.

†Assistant Research Professor, Department of Engineering and Applied Sciences; currently Visiting Professor, U.S. Air Force Academy, Astronautics Department.